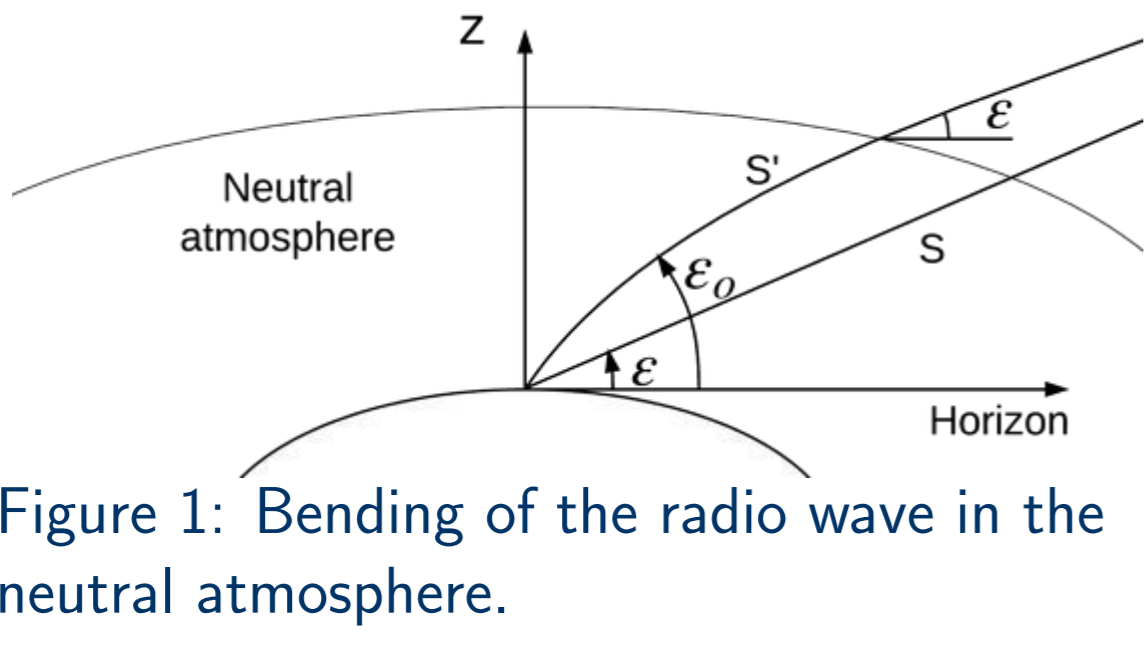


## Summary

The aim of this poster is to show the progress achieved in troposphere modeling using the The TOMographic Model of the IONospheric electron content (TOMION) software already functional for ionospheric and precise geodetic applications, as well as the dependencies on the sites coordinates with the tropospheric error.

## Introduction

When a radio wave travels through the lower atmosphere a delay is produced with respect to the time it would spend if traveling in the vacuum (S path in fig. 1).



The actual path (S') occurs when the medium produces a change in the refractive index. The tropospheric delay is commonly divided into two parts: hydrostatic and wet. Furthermore each component will be considered as the product of a zenith quantity and a function that projects this latter quantity into the line of sight, according to the elevation ε of the transmitter:

$$ZTD = ZHDm_h(\varepsilon) + ZWDm_w(\varepsilon), \quad [7] \quad \text{where}$$

$$ZHD = 10^{-6} K_1 R_h \frac{P_s}{g_m} \quad [9] \quad \text{and}$$

$$ZWD = 10^{-6} \left[ K_2' + \frac{K_3}{T_m} \right] \frac{g_m}{R_h} \frac{e_s}{(\Lambda + 1)g_m} \quad [1]$$

are the zenith tropospheric hydrostatic and wet delays; and m the corresponding Mapping Functions (MF). The parameters atmospheric surface pressure  $P_s$ , mean temperature of the column of air above the site  $T_m$ , water vapor pressure  $e_s$  and its decrease factor  $\Lambda$ , are to be determined for each site and epoch, while the constant for gases in hydrostatic equilibrium  $R_h$ , the mean gravitational acceleration of the column of air above the site  $g_m$ , and the refractivity values  $K_i$  are constants. MF involved in this work are Niell MF (NMF, [8]) and Vienna MF (VMF1, [2]). Both follow the same expression:

$$m(\varepsilon) = \frac{1 + \frac{a}{1 + \frac{b}{1 + c}}}{\sin(\varepsilon) + \frac{b}{\sin(\varepsilon) + c}}$$

but they differ in their way of computing the coefficients a, b and c, for both MF (wet and dry). VMF1 proposes in its fast version to obtain the  $a_h$  and  $a_w$  parameters through raytracing and  $b_{h,w}$  and  $c_{h,w}$  as follows:

$$b_h = 0.002905 \quad b_w = 0.00146$$

$$c_h = 0.0634 + 0.0014 \cos(2\varphi) \quad c_w = 0.04391$$

NMF has tabulated coefficients with a resolution of  $15^\circ$  in latitude,  $\varphi$ , independent of longitude. Their time variation and correction in height, for the epoch t, are described as:

$$x = x_{avr} + x_{amp} \cos\left(\frac{2\pi(t - T_0)}{365.25}\right) \quad \text{and} \quad \Delta m(\varepsilon) = \frac{dm(\varepsilon)}{dh} H$$

where  $T_0=28d$  is the phase

## Methodology: Data & Experiments

We have implemented VMF1 in TOMION software [5, 6] as another option to the already implemented NMF for 20 years. In fig. 2 we are schematizing the flow of implementation of

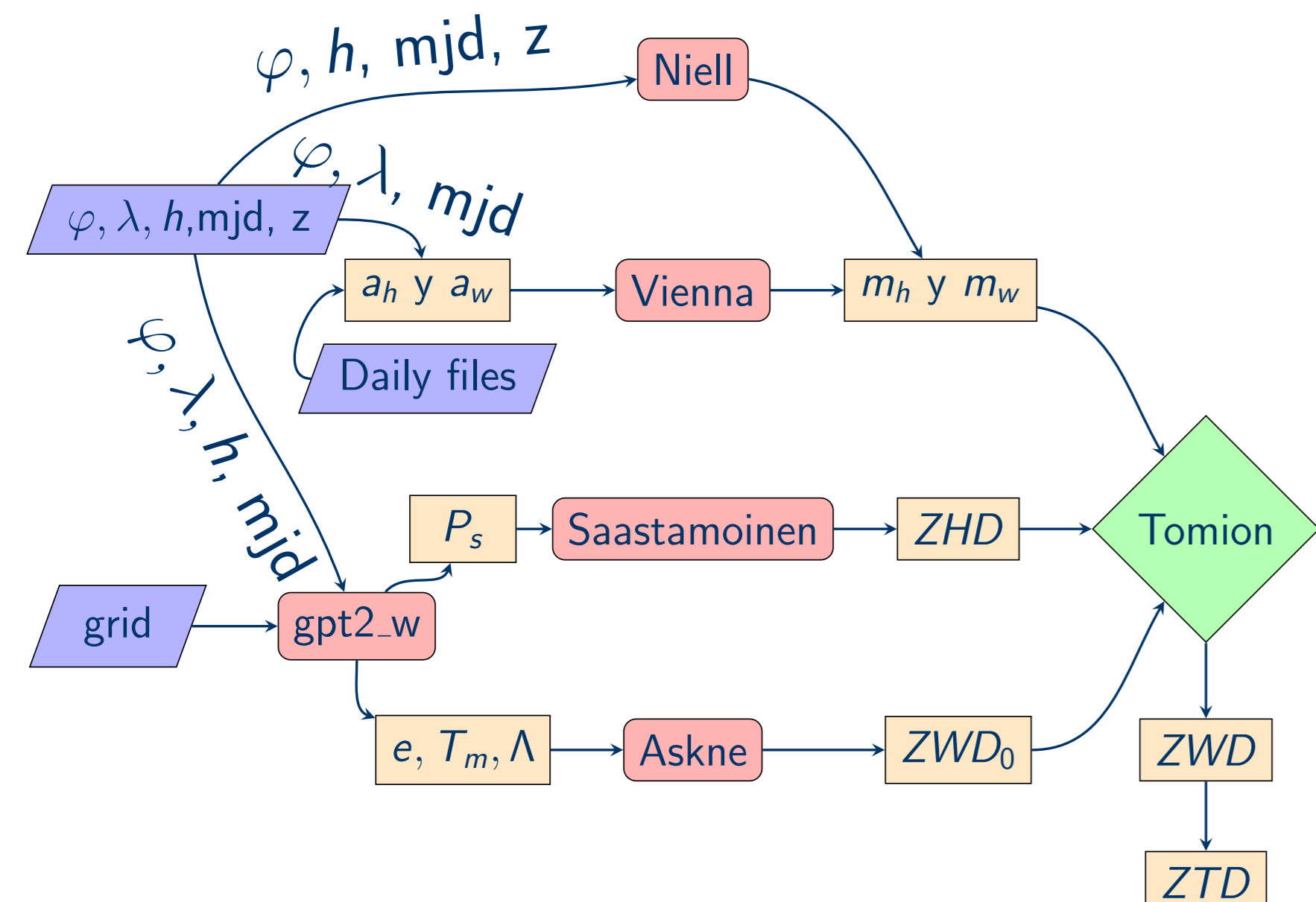


Figure 2: TOMION's Mapping Functions.

the new MF: as the processing begins, the software would automatically download the file from the web [4] for the corresponding date which contains the coefficients  $a_h$  and  $a_w$ . This coefficients will serve as input go the Vienna function that will give the parameters  $m_h$  and  $m_w$  that will later take part of the design of the matrix for the Kalman filter. On the other hand, it would also download the grid where temporal variations with annual and semiannual terms of the  $P_s$ ,  $T_m$ ,  $e_s$  and  $\Lambda$  parameters are modeled for each point with a resolution of  $1 \times 1^\circ$  and the subroutine *gpt2\_w* will perform the interpolation for the coordinates of the site. These four computed values are introduced in the computations of ZHD and ZWD, and used for the *prefit* of the filter again.

The data used for this work was GPS (Global Positioning System) pseudoangles in the ionospheric-free combination, both in Code and Phase ( $P_C$  and  $L_C$ ). The processing mode was Precise Point Positioning (PPP) and the corrections applied were: Geometric Range, Correction Clock, Instrumental Delays, Atmospheric Effects, Carrier Phase Wind-up Effect, Antenna Phase Centre Correction and Earth Deformation Effects, among others.

Experiment:

- ▶ Annual Run
- ▶ 8 IGS stations SE Australia
- ▶ Year 2014
- ▶ Reference: [site](#)

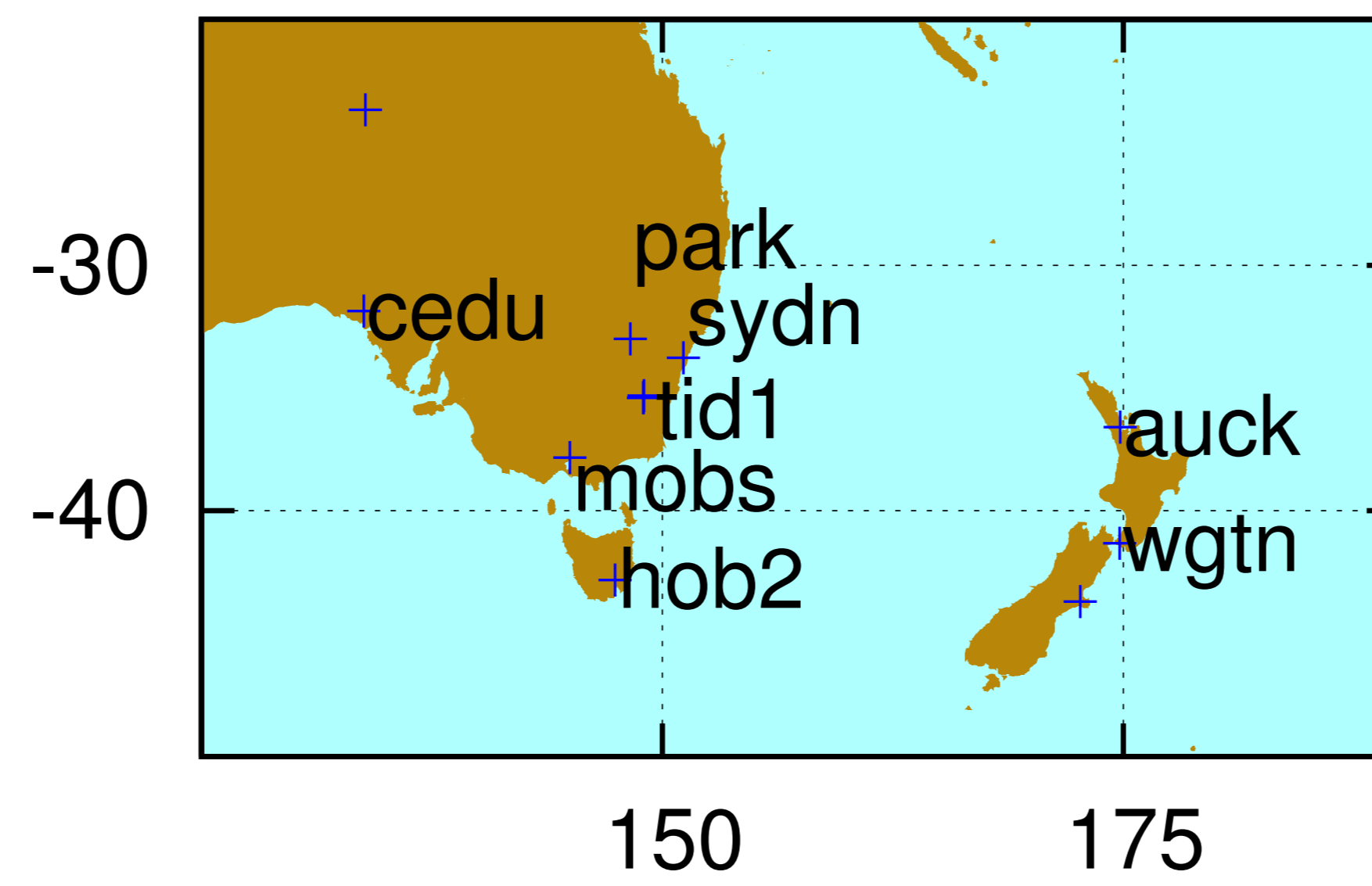
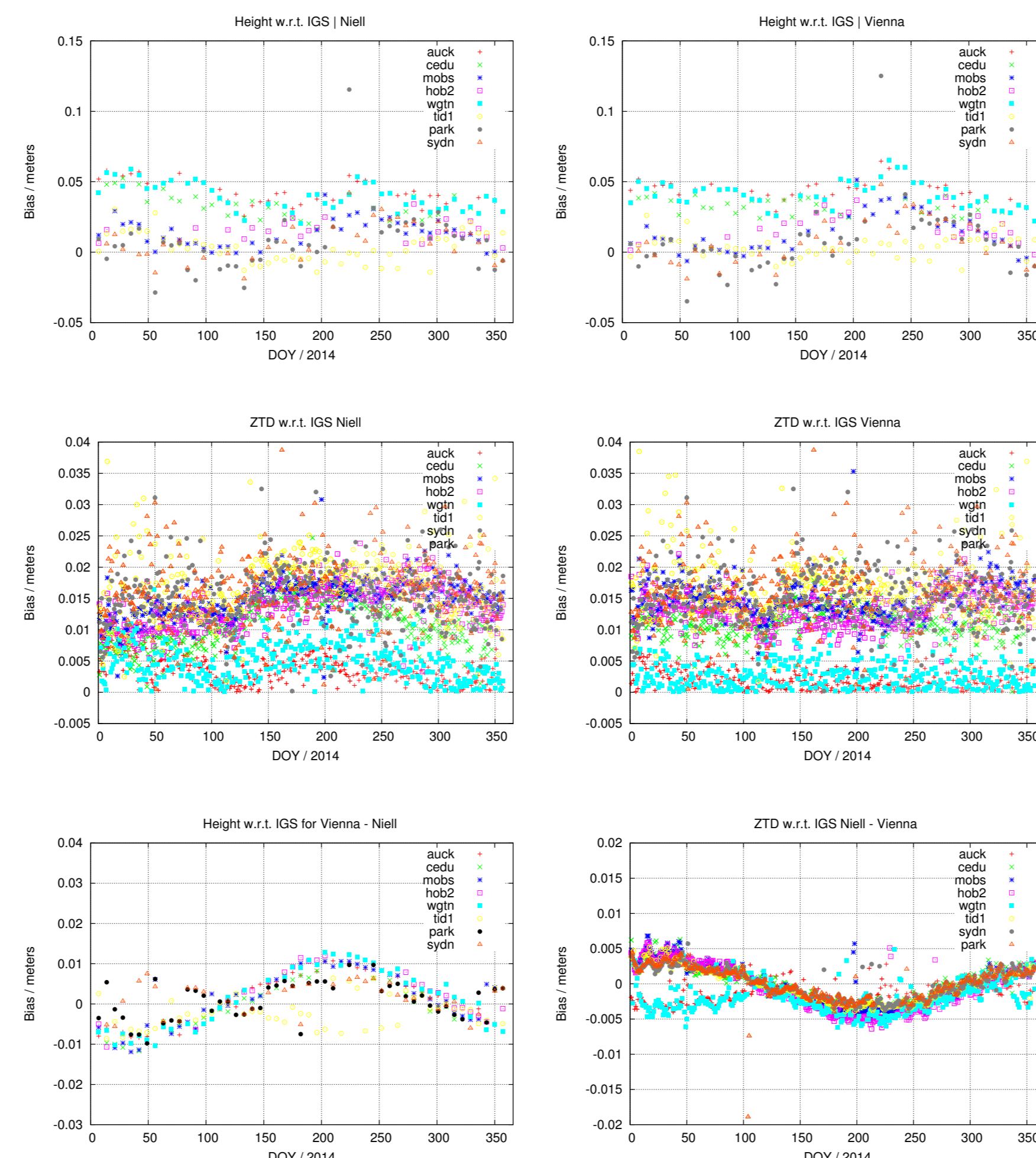


Figure 3: IGS Network used for the experiment.

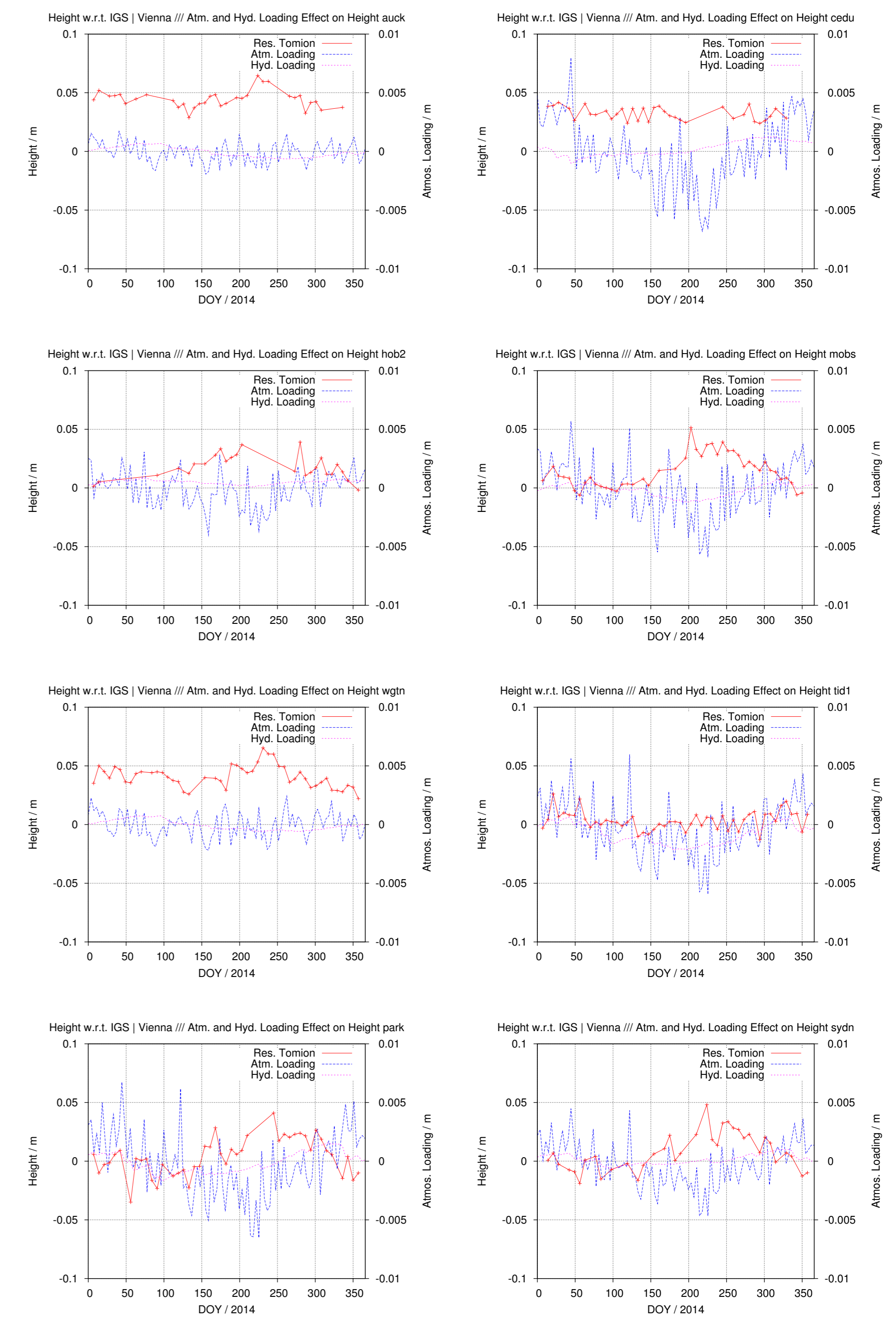
## Correlation of the site coordinates and the Zenith Tropospheric Delay

Figure 4: In this first overview of the performance of the new MF, we have considered the bias of the ZTD with respect to the IGS final troposphere product (middle left and right) and the corresponding departure of the site estimated height regarding the a priori value (top), taken from IGS as well. This figure shows that the ZTD is better estimated when VMF is applied while the coordinates take values further apart from the reference. The bottom plots show the difference of the residuals for the different MFs implemented for the ZTD (right) and the height (left).



## Effect of the Atmospheric and Hydrological Loading on the vertical coordinate

Figure 5: The weight of the atmosphere on the Earth surface as well as the hydrological mass induce deformations which can be detected on the coordinates displacement. We are showing here the effect on the height of the site of both loadings together with the residuals of the estimated coordinates with TOMION with respect to the IGS solutions, where the movement caused by the additional mass was computed using atmospheric, oceanic and hydrological general circulation models from the EOST Loading Service [3].



## Conclusions/Discussion

- ▶ The result of implementing a new troposphere mapping function in TOMION, Vienna MF (VMF1), led to a better estimation of the Zenith Tropospheric Delay.
- ▶ The use of Niell Mapping Function for projecting the ZTD into the line of sight can drive to a misinterpretation of the vertical coordinate of the site, in some of the cases.
- ▶ We have identified a potential correlation between the residual of TOMION's estimates of the height of the site and the displacement caused by the mass of the atmosphere and water on the Earth's surface, but further research regarding their relationship must be carried out.

## References

- [1] J. Askne and H. Nordius. Estimation of tropospheric delay for microwaves from surface weather data. *Radio Science*, 22(3):379–386, 1987.
- [2] J. Boehm and H. Schuh. Vienna mapping functions in vlbi analyses. *Geophysical Research Letters*, 31(1), 2004.
- [3] P. Gegout, J.-P. Boy, J. Hinderer, and G. Ferhat. Modeling and observation of loading contribution to time-variable gps sites positions. *Gravity, Geoid and Earth Observation*, pages 651–659, 2010.
- [4] GGOS. Global geodetic observing system, <http://ggosatm.hg.tuwien.ac.at/>, January 2017.
- [5] M. Hernández-Pajares, J. Juan, and J. Sanz. Neural network modeling of the ionospheric electron content at global scale using gps data. *Radio Science*, 32(3):1081–1089, 1997.
- [6] M. Hernández-Pajares, J. Juan, J. Sanz, and O. L. Colombo. Application of ionospheric tomography to real-time gps carrier-phase ambiguities resolution, at scales of 400-1000 km and with high geomagnetic activity. *Geophysical Research Letters*, 27(13):2009–2012, 2000.
- [7] T. Herring. Modeling atmospheric delays in the analysis of space geodetic data. *Proceedings of Refraction of Transatmospheric signals in Geodesy*, eds. JC De Munck and TA Spoelstra, Netherlands Geodetic Commission Publications on Geodesy, 36, 1992.
- [8] A. Niell. Global mapping functions for the atmosphere delay at radio wavelengths. *Journal of Geophysical Research: Solid Earth*, 101(B2):3227–3246, 1996.
- [9] J. Saastamoinen. Atmospheric correction for the troposphere and stratosphere in radio ranging satellites. *The use of artificial satellites for geodesy*, pages 247–251, 1972.